Palaeogeography, Palaeoclimatology, Palaeoecology 449 (2016) 385–396

Contents lists available at ScienceDirect

Palaeogeography, Palaeoclimatology, Palaeoecology

journal homepage: www.elsevier.com/locate/palaeo

Coral $\delta^{18}O$ evidence for Pacific Ocean mediated decadal variability in Panamanian ITCZ rainfall back to the early 1700s

Logan D. Brenner [a,b,*], Braddock K. Linsley [a], Robert B. Dunbar [c], Gerard Wellington [d,1]

[a] Lamont-Doherty Earth Observatory, Geoscience 104, 61 Route 9W, Palisades, NY 10964
[b] Department of Earth and Environmental Science, Columbia University, New York, NY 10027, USA
[c] Department of Environmental Earth Systems Science, Stanford University, Stanford, CA 94305, USA
[d] Department of Biology, University of Houston, Houston TX

ARTICLE INFO

Article history:
Received 25 June 2015
Received in revised form 22 January 2016
Accepted 1 February 2016
Available online 11 February 2016

Keywords:
Coral
Porites
Panama
Intertropical convergence zone
Pacific decadal oscillation

ABSTRACT

In Central America, seasonal and interannual shifts in the position of the Intertropical Convergence Zone (ITCZ) control the hydrologic budget. To better understand long-term changes in regional ITCZ-driven precipitation we re-examined a coral $\delta^{18}O$ record from a *Porites lobata* coral head near Secas Island (Core ID: S1) (7°59′ N, 82°3′ W) in the Gulf of Chiriquí on the Pacific side of Panamá. Linsley et al., (1994) originally published the 277-year time series and first described the presence of a narrow-band decadal cycle (period near 9–12 years) in $\delta^{18}O$. The original study did not present potential drivers for the decadal cycle, although they ruled out the influence of the sun spot cycle. Our re-analysis of this record supports the original interpretation that coral $\delta^{18}O$ is largely responding to variations in precipitation and associated river discharge, but with a new proposed mechanism to explain the decadal mode. There is no similar decadal cycle in gridded instrumental sea surface temperature from the area, suggesting that the decadal coral $\delta^{18}O$ signal results from hydrologic changes that influence coastal $\delta^{18}O_{seawater}$. The decadal component in S1 $\delta^{18}O$ is also coherent with a decadal mode embedded in the Pacific Decadal Oscillation (PDO) Index that we suggest has tropical origins. We speculate that the coral's temporary $\delta^{18}O$ deviation (1900–1930) in the decadal mode from the corresponding bands in rainfall and the PDO can be ascribed to a weak PDO in addition to local Panama gap wind variability and its effect on moisture transport from the Atlantic to the Pacific. Ultimately, the Secas Island coral $\delta^{18}O$ series records ITCZ-driven precipitation dictated by both the Atlantic and Pacific basins.

1. Introduction

Central American climate is strongly influenced by changes in the position of the Intertropical Convergence Zone (ITCZ). The ITCZ, a band of convecting atmospheric cells that encircles Earth, is located where the northern and southern trade winds converge near the equator (Philander, 1990; Schneider et al., 2014). Global precipitation is largely constrained by ITCZ position with its migration towards the warming hemisphere on seasonal and longer time-scales evident in both modern and paleoceanographic records (Schneider et al., 2014)(Fig. 1). In addition to seasonal shifts of the ITCZ, extratropical mechanisms such as the decadal-scale evolution of mid-latitude and equatorial Pacific Ocean surface ocean temperatures collectively referred to as the Pacific Decadal Oscillation (PDO), can influence ITCZ position (Schneider et al., 2014; Newman et al., in press).

The meridional movements of the ITCZ, particularly over Central America and more specifically the Pacific coast of Panamá, are responsible for seasonality in precipitation (Fig. 1). Although multiple climate models are able to reproduce these ITCZ movements, model dynamics are based on limited data and lack a long term observational context for evaluating the interannual and low frequency decadal and secular (long-term) variability underlying the typical seasonal shifts (Kumar et al., 2003; Soden and Held, 2006). There are few high-resolution seasonal reconstructions of ITCZ variability, and even fewer records extending back to the pre-industrial era. Coral-derived geochemical time series may be able to fill this data void by providing records of past precipitation on interannual and longer, low frequency time-scales.

The pronounced rainfall gradient associated with seasonal meridional ITCZ oscillations over the Gulf of Chiriquí combined with very low amplitude annual sea surface temperature (SST) variability make this region an excellent location to study long-term precipitation patterns using coral skeletal oxygen isotope analyses ($\delta^{18}O$). Coral $\delta^{18}O$ is known to be primarily influenced by both SST and the $\delta^{18}O$ of the seawater, which is linearly related to local sea surface salinity (SSS)(Fairbanks et al., 1997). In some regions, like the Gulf of Chiriquí, precipitation and river discharge lead to seawater $\delta^{18}O$ variability that has a significantly greater effect on

* Corresponding author at: Lamont-Doherty Earth Observatory, Geoscience 104, 61 Route 9W, Palisades, NY 10964.
E-mail address: lbrenner@ldeo.columbia.edu (L.D. Brenner).
[1] (Deceased)

http://dx.doi.org/10.1016/j.palaeo.2016.02.001
0031-0182/

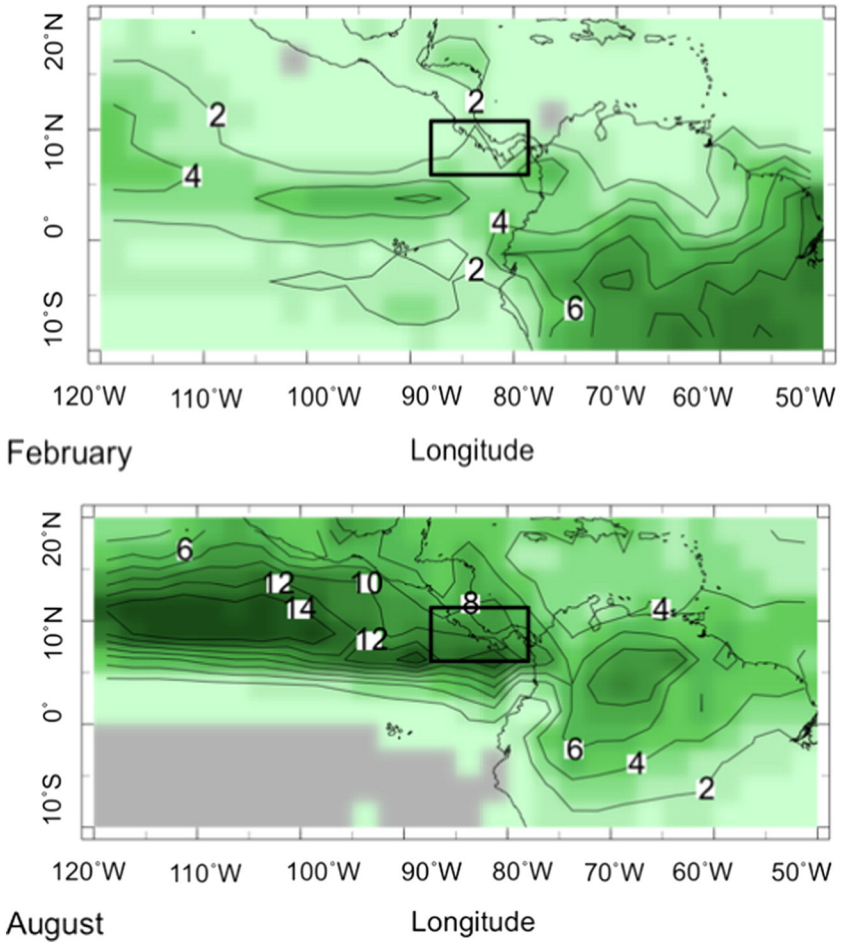

Fig. 1. Seasonal meridional shifts in ITCZ position control the duration and strength of the Central American wet season. Contours represent bands of equal rainfall (mm). The darker green region shows an area of high precipitation representing the location of the ITCZ. The band travels north towards Panamá in the boreal summer (lower panel). Our study site is located within the black box off the Pacific coast of Panamá. (Modified from Xie and Arkin, 1996, 1997).

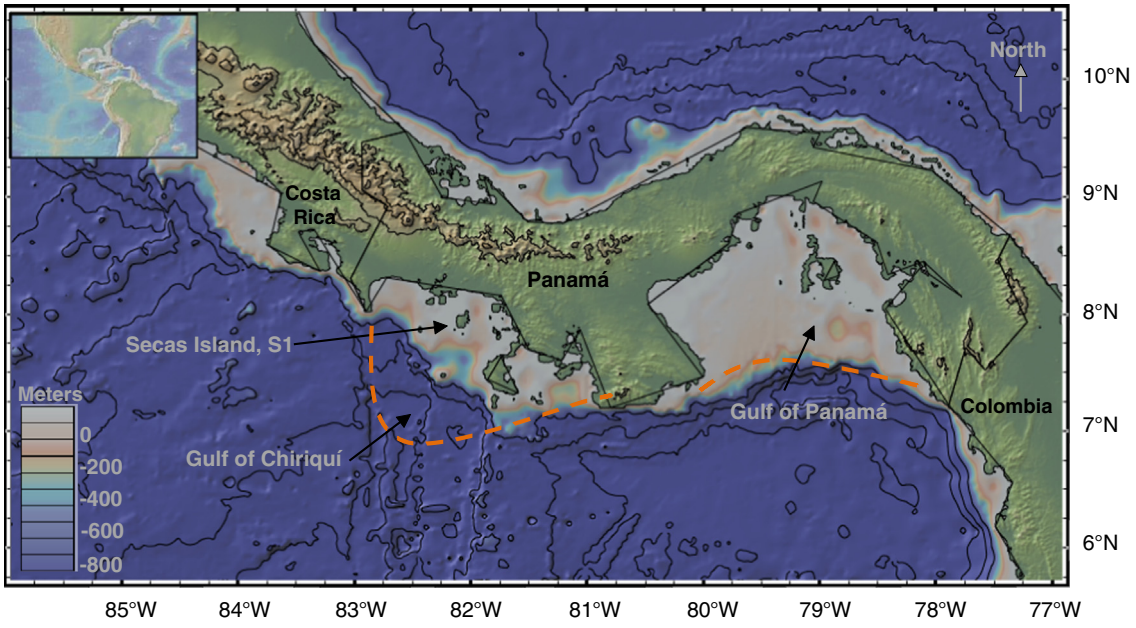

Fig. 2. The Isthmus of Panamá and coral study site at Secas Island (7°59′ N, 82°3′ W) with 1000 m contours. Secas Island is located within the Gulf of Chiriquí. The dotted lines outline the approximate boundaries of the major gulfs along the Pacific coast of Panamá. The North Equatorial Counter Current flows eastward towards the isthmus and Gulf of Chiriquí. Ocean currents also flow westward, away from the isthmus, in the Gulf of Panamá while the Gulf of Chiriquí remains calmer.

coral $\delta^{18}O$ than the approximately −0.23 ‰/°C effect of SST (Epstein et al., 1953). Corals from this setting may provide a unique means for studying regional hydroclimate that is directly related to the ITCZ. Previous $\delta^{18}O$ analyses conducted on a *Porites lobata* coral core from Secas Island, Panamá, in the Gulf of Chiriquí, elucidated decadal (9–12 years) variability in its $\delta^{18}O$ record spanning 1707–1984 CE (Coral ID: S1) (Fig. 2) (Linsley et al., 1994).

However, no potential mechanisms for this cycle were presented in the original publication leaving the source of the variability and its potential impacts unexplored. Here we will present evidence that the decadal component in coral $\delta^{18}O$ in the Gulf of Chiriquí tracks decadal changes in the Pacific spatial SST field via its influence on both wet and dry season rainfall. The PDO is defined as the leading principal component of North Pacific monthly SSTs north of 20°N (from 1900 to 1993). The positive and negative PDO index track anomalously warm or cool conditions in the North Pacific, respectively, with basin wide impacts on ecology, precipitation, and temperature. A recent assessment by Newman et al. (in press) indicates that the PDO is a confluence of basin-wide phenomena whose combined tropical and north Pacific forcings equate to the SST anomalies characteristic of the PDO. The three major processes that comprise PDO variability include: 1) ocean surface heat flux related to stochastic local weather driven by the Aleutian low, 2) ocean thermal inertia as "re-emergence" coined ocean memory, and 3) decadal variability in the Kuroshio-Oyashi current (Newman et al., in press). In particular, the ocean heat flux and Ekman (wind-driven) transport driven by stochastic local weather is linked through the atmospheric bridge to interdecadal and decadal ENSO forcing (Newman et al., in press). Ultimately, the PDO is a complex system of forcings and climate modes acting across a spectrum of timescales. Therefore, delineating how or why the PDO or its impacts influences a certain region becomes complex. Our analysis suggests that a tropically forced decadal mode embedded within north Pacific SST, which is one component of the PDO Index (see Newman et al., in press), appears to be related to the narrow-band of decadal variability in our S1 coral $\delta^{18}O$ record by regulating Panamanian precipitation on that same timescale.

2. Modern Panamanian climate

During the boreal summer the ITCZ migrates northward to between 8° N and 12° N stimulating the Panamanian wet season from May–November, with maximum rainfall in September, while its southward retreat in the boreal winter leaves the region dry from December–April (Horel, 1982; Linsley et al., 1994) (Fig. 1). Total wet season rainfall amounts to 2000–3000 mm, whereas precipitation during the dry season only totals 200–500 mm, thereby setting up a stark precipitation gradient associated with the meridional ITCZ movement (Poveda et al., 2006; Lachniet, 2009; Valiela et al., 2012) (Fig. 3B). Additionally, Panamá's monthly precipitation data clearly depicts consistent seasonal precipitation oscillations with only one annual maximum, suggesting that, at least since the early 1900s, the ITCZ has not moved significantly north of Panamá.

Zonal atmospheric convection patterns (Walker Circulation) also influence precipitation in Panamá. Instrumental precipitation data from several sites in Panamá show clear impacts of ENSO. Interannual variability in tropical paleoclimate records can often be attributed to individual El Niño and La Niña events, which have a recurrence interval of 3–8 years, and depending on the location can be characteristic of

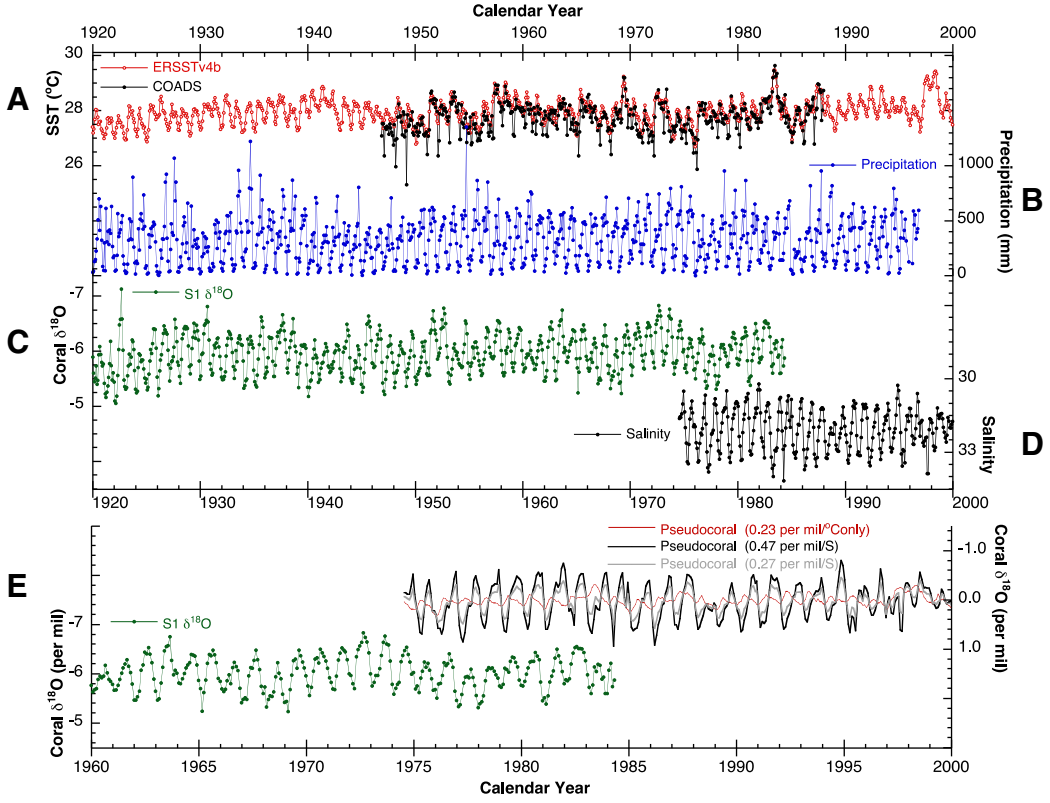

Fig. 3. A) Two SST records centered near the Gulf of Chiriquí (8°N, 82°W) from the ERSST (red) and ICOADS (black) databases are shown. The SST annual cycle is small and irregular with an average annual amplitude of only ~1 °C. **B)** A monthly precipitation dataset from the University of East Anglia's Climatic Research Unit (UEA CRU) (2.5°lat × 3.75°long grid) centered over the Gulf of Chiriquí (7.5°N, 82.5°W) shows a much larger annual cycle with dry season precipitation as low as 200 mm and the wet season yielding as much as 5,000 mm (data from Hulme, 1992; Hulme, 1994). **C)** Like the precipitation record, subannually resolved coral $\delta^{18}O$ from S1 (green) also follows a clear and consistent annual cycle of ~1 ‰. **D)** The salinity record also exhibits seasonality driven by the precipitation from a quadrant encompassing the Gulf of Chiriquí (7.5°N, 82.5°W) (data from Delcroix et al., 2011). **E)** In order to assess the contribution of precipitation and SST on coral $\delta^{18}O$ variability we created 3 pseudo corals based on SST and SST + SSS sensitivities (red, black, gray) compared to the coral $\delta^{18}O$ (green). The coral $\delta^{18}O$ response to SST is swamped by the precipitation signal, producing the most accurate pseudocorals when the SSS response is taken into account.

drought or extreme rainfall rivaling the wet-dry season contrast (Cole et al., 1993; Urban et al., 2000; Cobb et al., 2013). Under El Niño conditions, Panamá becomes relatively dry with anomalously elevated SSTs as the ITCZ remains in a more southerly position (Ropelewski and Halpert, 1987, 1989; Kiladis and Diaz, 1989).

In addition to the impact of Walker Circulation and Hadley Cell dynamics on the position of the ITCZ, cross-isthmus gap wind variability also influences Central American climate. The Central American Cordillera focuses drainage of ITCZ-driven rainfall into the Gulf of Chiriquí and partially blocks the trade winds, limiting upwelling and therefore minimizing seasonal SST variability (Duque-Caro, 1990; Glynn, 1977). The gap winds also modulate air temperature in Panamá creating cooler conditions along the Pacific side during the dry season when winds blow westward across the isthmus (D'Croz and O'Dea, 2007, 2009). Although the winds can create subtle spatial variability in temperature, the country's near-equatorial location and topographic trade wind blocking limit temporal variability with temperatures hovering around 30 °C. SSTs are also relatively invariant throughout the year, averaging ~28 °C in the Gulf of Chiriquí with an average annual amplitude of ~1 °C compared to the neighboring Gulf of Panamá with a 4–8 °C annual amplitude (Glynn, 1977; Linsley et al., 1994; Alory et al., 2012; Wade McGillis pers. Comm.) (Fig. 3A). The eastward flowing North Equatorial Counter-Current (NECC) dominates offshore conditions in the Gulfs of Panamá and Chiriquí with westward wind-driven flow away from the coast abutting the Gulf of Panamá. The dissimilarity in SST variability between the two gulfs underscores the differences in their respective upwelling regimes.

Unlike SST, sea surface salinity (SSS) (all salinity measurements reported based on the Practical Salinity Scale of 1978, PSS-78) in the coastal waters along Pacific Panamá exhibit a large annual amplitude of about 3 owed to the seasonal shifts in the ITCZ and resulting variability in rainfall and river discharge (Delcroix et al., 2011; Alory et al., 2012) (Fig. 3D). During the dry season about half of the precipitation in the region is derived from the Atlantic when the ITCZ is located in its more southerly position and when strong northeasterly trade winds carry Caribbean-sourced water vapor over the isthmus towards the Pacific (Benway and Mix, 2004; Prange et al., 2010). In addition to the meteoric freshwater input, a series of 8 watersheds along the Pacific coast of Panamá drain into the Gulf of Chiriquí and can directly influence local SSS (Valiela et al., 2012). While seasonal SST variability within the inner reaches of the Gulf of Chiriquí is greatly reduced relative to the Gulf of Panamá due to geographic blocking of the seasonal trade winds, SSS is more similar with large amplitude seasonal freshening of 2.5 and 2.1 in the Gulf of Chiriquí and Gulf of Panamá, respectively. The SSS at the mouths of the estuaries ranges from as low as 20 during the wet season to 31–34 during the dry season, which is similar to ambient surface seawater in the Gulf of Chiriquí, during the dry season (Valiela et al., 2012). The freshwater discharge extends into both the Gulf of Chiriquí and Gulf of Panamá out to ~300 km during the wet seasons, effectively amplifying the precipitation signal recorded by coral $\delta^{18}O$ in the region (Linsley et al., 1994).

Alory et al. (2012) investigated the seasonal dynamics of this eastern Pacific fresh pool using complementary satellite wind, rain, sea level and in situ oceanic current data at the surface, along with hydrographic profiles. Their observations depicted the quasi-permanent presence of a far eastern Pacific fresh pool with SSS lower than 33, which is confined between Panama's west coast and 85°W in December and extends to 95°W in April. The fresh pool appears off Panamá due to the strong summer rains associated with the northward migration of the ITCZ over Central America in June. The eastward-flowing NECC traps the fresh pool against the coast and strengthens the SSS front on its western edge. As the ITCZ moves southward in the winter, the northeasterly Panama gap wind creates a southwestward jet current in its path. As a result, upwelling in the Panamá Bight brings cold and salty waters to the surface that erode the fresh pool on its eastern side while the jet current and the enhanced South Equatorial Current stretch the fresh pool westward until it nearly disappears in May. The relatively stable SSTs in the Gulf of Chiriquí combined with the large influence of ITCZ-related precipitation and river discharge on surface salinity makes it a unique study site for using coral $\delta^{18}O$ to evaluate past changes in hydroclimate.

3. Methods

3.1. Coral Core Study site and sample preparation

The Secas Island (S1) core was collected from a living massive *Porites lobata* coral head in June of 1984 by Secas Island (7°59′ N, 82°3′ W), 25 km south of mainland Panamá in the Gulf Chiriquí, Panamá (Fig. 2). The S1 coral head was located at 3 m water depth and the core totaled 2.8 m in length. As discussed in Linsley et al. (1994), the cylindrical core was cut perpendicular to the coral growth bands into 7 mm thick slabs using a water-cooled rock saw. The slabs were cleaned in deionized water and were X-rayed in a Philips Radiflour medical X-ray unit (at 35 Kv). The X-ray positives elucidated the density couplets used to identify the maximum growth axis, which served as the sampling pathway down the entire core (Fig. 4). Subannual $CaCO_3$ samples were hand-drilled down core at 1 mm intervals by excavating a 2 mm wide by 2 mm deep trough.

3.2. Age model and chronology development

The X-ray positives of the Secas Island core revealed clear alternations of low- and high-density annual growth bands (Fig. 4)(Linsley et al., 1994). *Porites* from the Gulf of Chiriquí secrete low-density bands during the dry season when photosynthetic rates increase due to decreased cloud cover, less frequent storms and increased solar radiation reaching the sea surface (Linsley et al., 1994; Glynn, 1983; Wellington and Glynn, 1983). The elevated photosynthesis increases skeletal extension rates, thereby forming low-density coral skeletal aragonite. During the wet season, photosynthesis generally decreases due to ITCZ-driven storms and higher cloud cover. The decreased photosynthesis rate leads to a lowered extension rate, which could also be a stress response to lower salinities, and results in thicker skeletal elements (higher density growth bands) at those times.

The S1 $\delta^{18}O$ record spans 277 years from 1707 to 1984 CE with a total of 2,739 discrete samples. There is a clear ~1.0 ‰ annual $\delta^{18}O$ cycle and an average growth rate of ~11 mm/year. After considering the timing and impact of precipitation and river discharge on skeletal aragonite $\delta^{18}O$, Linsley et al. (1994) attributed the lowest coral $\delta^{18}O$ value in a given year to the month corresponding with the greatest amount of rainfall that year. The final time series was developed using the ARAND software package (Howell et al., 2006). In this study we have re-interpolated the S1 time series to 12 points per year, rather than 10 points as was done in the original publication (Linsley et al., 1994). Because our interest here was to further investigate the decadal-scale variability in this record, calendar year annual average $\delta^{18}O$ was calculated from the subseasonal data prior to further time series analysis. Based on the time series we also created annual average wet and dry season values. Although the dry season spans part of two calendar years (November/December–April) for analytical purposes, the year of the dry season was attributed to the year in which it started.

3.3. Analytical methods

The S1 coral powders were dissolved in ~100% H_3PO_4 at ~50 °C and the resulting CO_2 gas analyzed on a VG Micromass 602E mass spectrometer at Rice University (see Linsley et al., 1994). The entire core was analyzed with 15% sample replication with a replicate standard deviation of 0.053 ‰. In addition, the National Institute of Standards and Technology (NIST)-20 standard was analyzed 2–3 times per run yielding a $\delta^{18}O$ standard deviation of 0.067 ‰.

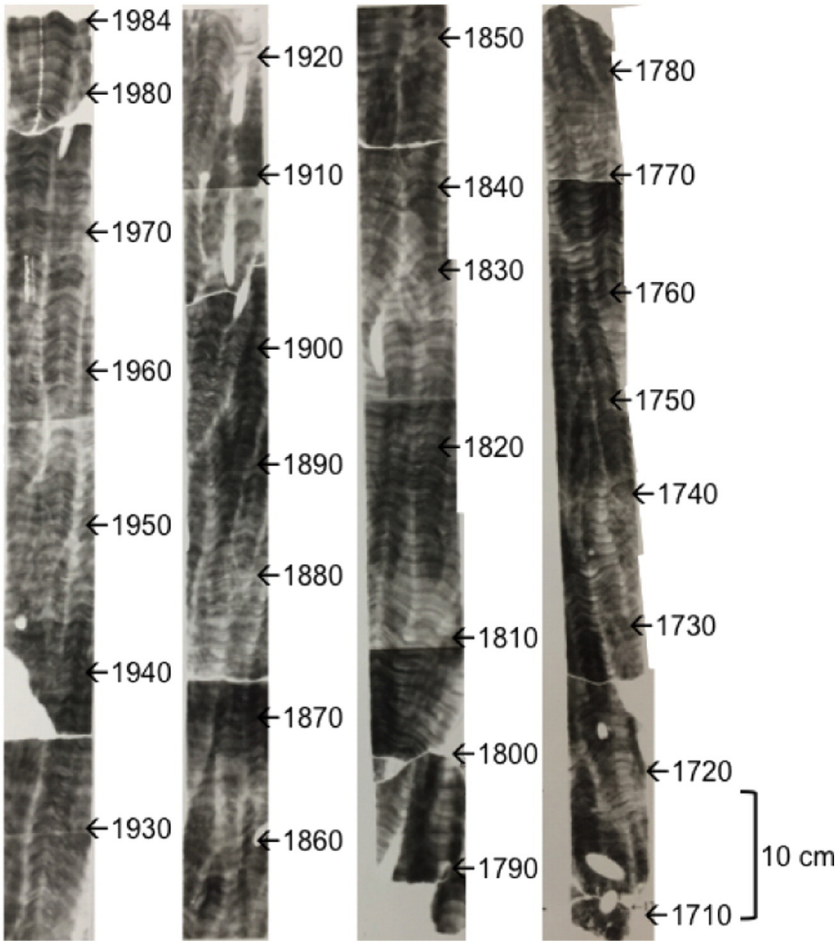

Fig. 4. X-Ray positive collage of S1 with approximate age model. The light bands represent less dense skeletal elements (dry season) due to increased photosynthetic rates from a lack of storm-related cloud cover. A light and dark band couplet represents a year of growth.

In this study we used singular spectrum analysis (SSA) to isolate and evaluate the various oscillatory modes in the annual average S1 time series with the ssaX program, written and compiled by E. Cook at the Lamont-Doherty Earth Observatory Tree Ring Laboratory. We varied the window length (M-value) on multiple SSA runs to identify the stable eigenvectors. Previously described by Linsley et al. (1994), this analysis revealed a stable set of narrow-band modes with mean periods between 9 and 12 years (Table 1). The SSA procedure is described in earlier studies presented by Fukunaga (1970); Vautard and Ghil (1989), and Vautard et al. (1992). To determine the correlation of various time series we used the Pearson product–moment correlation and accounted for reduced degrees of freedom from the annual averages. Correlation coefficient descriptors (e.g. weak, moderate, strong) were applied according to the guidelines set forth by Evans (1996).

3.4. Coral $\delta^{18}O$ interpretation

The seasonal SST variability is weak and irregular relative to the large amplitude in seasonal variability of rainfall and SSS in the Gulf of Chiriquí. Therefore we conclude, as did Linsley et al. (1994), that the ~1 ‰ seasonal cycle amplitude in coral $\delta^{18}O$ is largely driven by seasonal changes in precipitation and the consequent change in $\delta^{18}O_{seawater}$. To support this assertion we created 3 pseudocoral $\delta^{18}O$ records using instrumental data: one based solely on SST and two based on SST and SSS with different SSS sensitivities (Fig. 3C, E).

The monthly SST data was acquired from the International Comprehensive Ocean–Atmosphere Dataset (ICOADS) and the Extended Reconstructed Sea Surface Temperature (ERSST) over the Pacific region (82°W, 8°N) of Panamá indicated a small, sporadic annual SST cycle with an average SST of 28° and an average annual amplitude of 1° (Fig. 3A). The SSS data was taken slightly offshore (7.5°N, 82.5°W) from the Delcroix et al. (2011) gridded SSS database. Because the regional SSS data, upon which the pseudocoral $\delta^{18}O$ was derived, appears to be largely driven by rainfall and river discharge over the area, we compared our coral data to two precipitation databases: a monthly resolution record from the University of East Anglia's Climatic Research Unit (UEA CRU) (2.5°lat × 3.75°long grid) centered over the Gulf of Chiriquí (7.5°N, 82.5°W) back to 1900 and an annual average record from a composite of 4 Pacific coast rain gauges to provide a regional representation back to 1856.

The pseudocoral modeling exercise indicates that the average annual amplitude in coral $\delta^{18}O$ attributed to SST variability (based on ERSST) is 0.26 ‰ and its influence on coral $\delta^{18}O$ is offset by several months from the influence of salinity (see Fig. 3E). The addition of the SSS data converted to per mil space via commonly accepted global and tropical $\delta^{18}O$-SSS sensitivities (0.47 and 0.27 ‰/S, respectively) yielded a pseudocoral $\delta^{18}O$ annual amplitude similar to the S1 record, even if we disregard the SST contribution (Fig. 3E). Therefore, we attribute the majority of the variability within the $\delta^{18}O$ annual cycle to oscillations in precipitation and river discharge as concluded by Linsley et al. (1994), re-affirming the age model development process of associating annual $\delta^{18}O$ minima with rainfall maxima.

Table 1
Summary of SSA results and associated variances from annually averaged and seasonally averaged records. The top 10 eigenvectors are provided. The decadal RCs are the sums of all eigenvectors with average modes of 9–12 years. Note that the decadal mode in annual average S1 δ^{18}O incorporates eigenvectors 15 and 16 both with average modes of 11 years.

Annual average S1 δ^{18}O			Annual average precipitation		
Eigenvector	Period (yr)	Variance (%)	Eigenvector	Period (yr)	Variance (%)
1, 2	9	10	1,2	4	17
3, 4	19	9	3, 4	15	12
5	42	4	5, 6	3	11
6	48	4	7, 9	9	9
7, 8	7	8	8	2	5
9	91	4	*Decadal*	*9*	*9*
10	27	3			
Decadal	*10*	*15*			

Wet season S1 δ^{18}O			Dry season S1 δ^{18}O		
Eigenvector	Period (yr)	Variance (%)	Eigenvector	Period (yr)	Variance (%)
1, 2, 5	9	27	1	10	8
3	32	10	2	9	7
4	19	8	3	36	8
6	11	7	4	18	7
7	77	6	5, 6	7	12
Decadal	*10*	*34*	7	16	6
			8	91	6
			Decadal	*10*	*15*

Annual average PDO		
Eigenvector	Period (yr)	Variance (%)
1	53	13
2	50	10
3, 4	6	14
5	26	6
6	19	6
7, 8	9	8
Decadal	*9*	*8*

4. Results

The S1 δ^{18}O record exhibits clear seasonal variations, identified by a single peak (δ^{18}O minima) during Panamá's wet season (Fig. 5). Throughout the entirety of the δ^{18}O record the average annual amplitude is 0.85 ‰ with a standard deviation of 0.21 ‰ and a secular (long-term) trend with an amplitude of 0.30 ‰ towards more deplete values.

We used SSA to separate the dominant temporal modes in S1 coral δ^{18}O into reconstructed components (RC). An analysis of the raw data showed that, as expected, the annual cycle in coral δ^{18}O accounted for ~50% of the total variance. In order to more closely examine lower frequency oscillations we calculated an annually averaged S1 δ^{18}O series from the subseasonal data and re-ran SSA on the raw and detrended versions of the data. Both analytical approaches resulted in similar results for the decadal and interannual bands but we report the SSA analysis of the detrended annual average S1 δ^{18}O data. In this study the decadal mode is defined as the sum of all eigenvectors with average modes of 9–12 years to provide a 2-year bookend around the 10-year mark without entering into the typical El Niño band.

The SSA of the annual average S1 coral δ^{18}O record showed that 15% of the variance is in the decadal band and primarily associated with a pair of RC's in quadrature with a mean period of 9 years (Table 1, Fig. 6). To assess regional rainfall variability we applied SSA to the composite regional annual average precipitation record we generated back to 1856, which also yielded a narrow decadal band (9–12 years) responsible for 9% of the variance following an ENSO mode (~20%) mode (Table 1). The decadal mode in annual average precipitation is well correlated to annual average coral δ^{18}O decadal RCs with a moderate correlation coefficient of $R = -0.58$ ($p < 0.001$) from 1984 back to 1930 (Table 2; Fig. 6A). Prior to 1930 our precipitation composite drops from an average of 4 locations to just 2 and therefore may be biased before 1930.

To further evaluate S1 coral δ^{18}O variability we detrended separate annual average δ^{18}O records for the wet and dry seasons to examine season-specific variability over time (Fig. 7). A comparison of the detrended wet and dry season δ^{18}O values within the same year are directly correlated, $R = 0.58$ ($p < 0.001$) for the entire record (Table 2). Both the wet and dry season δ^{18}O records contain decadal-scale oscillations responsible for 34% and 15% of the total variance, respectively. The amplitude of the decadal cycles in the wet and dry seasons are largely in accord with one another, with the exception of a brief period from about 1920–1935 and 1850–1865 when the δ^{18}O dry season amplitude is small and irregular in comparison to the corresponding wet season. This is the same interval over which the decadal RC in precipitation is misaligned with the decadal RC in coral δ^{18}O. All correlations involving the annual and seasonal average records from the coral decadal mode are provided in Table 2.

5. Discussion

5.1. Assessing the SST and precipitation signals in the coral δ^{18}O records

Based on all available data, we suggest that in this unique setting seasonal and decadal variations in coral δ^{18}O are strongly influenced by changes in ITCZ-driven rainfall and the consequent river runoff into the Gulf of Chiriquí. Assuming a -0.23 ‰ δ^{18}O per 1°C of SST increase (Epstein et al., 1953; Wellington et al., 1996) the annual SST signal results in an irregular oscillation, only contributing ~20% of average annual coral δ^{18}O variability. Our pseudocoral records suggest that seasonal coral δ^{18}O is largely affected by precipitation and river discharge

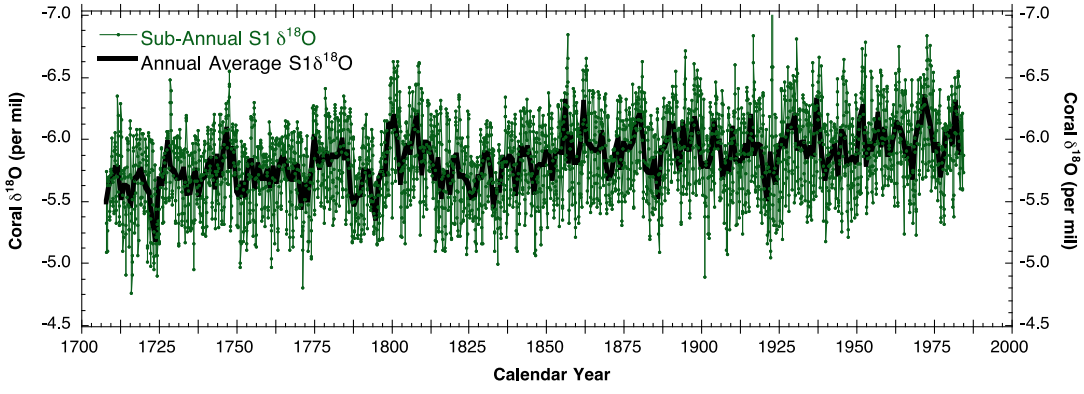

Fig. 5. Complete S1 δ^{18}O time series (green) (12 pts./year) and annual average record (black) from 1707.7–1984.3 CE. The S1 δ^{18}O time series was originally interpolated to 10 points per year and published by Linsley et al. (1994). S1 appears to record both annual and interannual variability. Note the inverted y-axes with more depleted δ^{18}O values representing wetter conditions oriented towards the top.

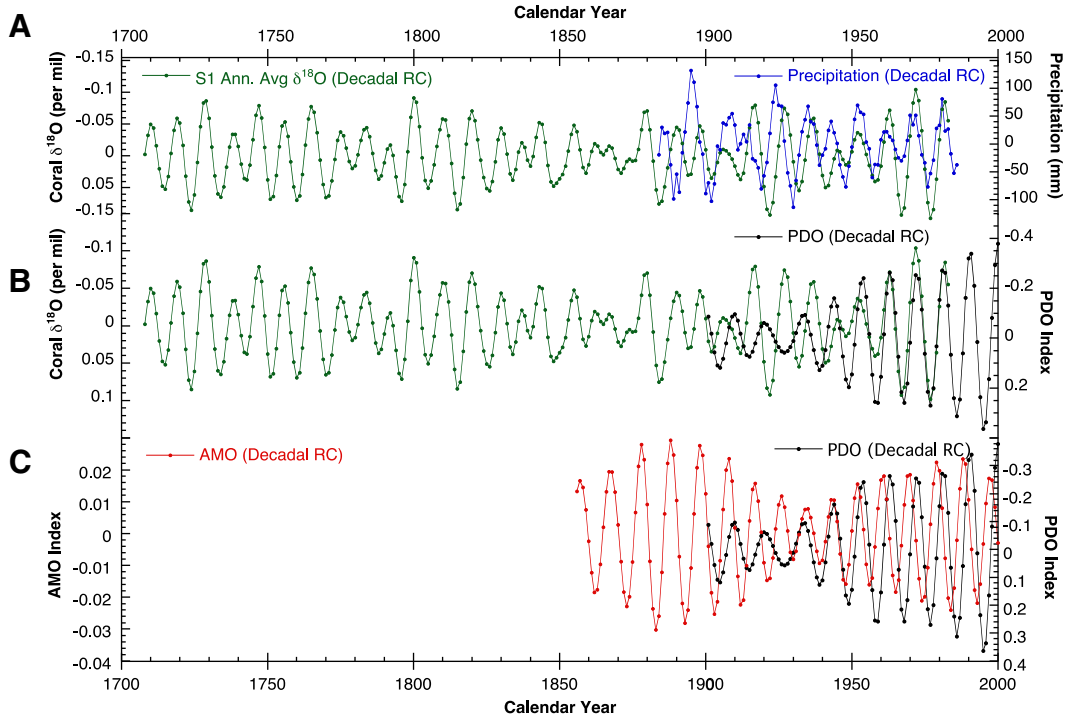

Fig. 6. A) The time evolution plot of the decadal RCs of the detrended annual average $\delta^{18}O$ record from Secas Island (green) and the decadal RC of the annually averaged multi-station composite of regional Pacific coast precipitation (blue). The two records are directly correlated yielding a correlation coefficient of $R = -0.58$ from 1930 to present, supporting our assertion that coral decadal $\delta^{18}O$ responds to precipitation variability in that same band. Before 1930 the relationship between S1 and rainfall weakens and becomes less clear. **B)** The decadal phases in S1 $\delta^{18}O$ and the PDO yields a correlation coefficient of $R = -0.62$ from 1984 back to 1930 and $R = -0.42$ for the entirety of the record. The relationship suggests that the DPDO, and hence spatial SST pattern in the Pacific, influences Panamanian precipitation in that same band, which is recorded in Secas Island coral $\delta^{18}O$. **C)** A comparison of the decadal bands extracted from the PDO and AMO indices. The PDO index is inverted with negative PDO excursions associated with more rainfall. The two records are generally in accord from present back to 1930. However, from 1930 to 1900 the two records, created with independent chronologies, suggest a period of disorganization in the regional hydroclimate, which could be responsible for the period of asynchrony between coral $\delta^{18}O$ and rainfall shown in the top panel.

(Fig. 3E). While the SST history from the Gulf of Chiriquí is difficult to decipher using coral $\delta^{18}O$, the pronounced seasonal precipitation gradient made for an excellent opportunity to reconstruct ITCZ-driven rainfall and runoff.

As was mentioned earlier, a unique aspect of the S1 study site at Secas Island is its protection from the wind driven upwelling that defines the nearby Gulf of Panamá. The heterogeneous nature of Panamá's Pacific coast is evident in the varied conditions between the Gulf of Chiriquí and the Gulf of Panamá (Fig. 8). The Central American Cordillera abutting the Gulf of Chiriquí effectively blocks the westward flowing "gap winds" that drive the upwelling of cool waters in the neighboring gulf (see Alory et al., 2012). More specifically, during the boreal winter the ITCZ shifts southward allowing the northeasterly Panamanian gap winds to develop a southwestward jet (Alory et al., 2012). The gap wind-driven jet elicits Ekman pumping in its wake, resulting in strong upwelling in the Panamá Bight, replacing the eastern tropical Pacific warm pool with cold, saline water (Alory et al., 2012). Since Secas Island is located in the heart of the Gulf of Chiriquí where SSTs do not have a distinct seasonal cycle we are able to interpret the coral $\delta^{18}O$ record without the influence of upwelling.

The mean annual skeletal $\delta^{18}O$ contains a small secular trend towards lower $\delta^{18}O$ values in the 20th century. The S1 coral exhibited a decrease of 0.30 ‰ with most of the change occurring from 1830 to 1860 (see Linsley et al., 1994). The original interpretation, based on our established relationship between coral $\delta^{18}O$ and precipitation, is that coral $\delta^{18}O$ reflects a shift towards a wetter hydroclimate over Pacific Panamá (Linsley et al., 1994). More notable is that the amplitude of the secular trend is smaller than those found in other tropical Pacific *Porites* $\delta^{18}O$ records (e.g. Dassié et al., 2014; Linsley et al., 2006). We speculate that the secular trend in coral $\delta^{18}O$ is largely a measure of a SSS change (decrease) of 0.6–1.1 (global vs. tropical $\delta^{18}O$-SSS relationships). Linearly extrapolating instrumental SSS to 1707 to extend the record as far back as the coral $\delta^{18}O$ series extends, yields a long-term change of ~1.6, slightly larger than our calculated value. The secular trend amplitude would have to be larger if it were to incorporate SST in addition to the SSS variability. The lack of an SST influence may explain why the S1 secular trend is smaller than those found in most other Pacific *Porites* $\delta^{18}O$ records.

Table 2
Summary of the Pearson product–moment correlations (R-values) calculated with S1 annual and seasonal average decadal scale data. The R-values were calculated over the time period from 1983 to 1930. We truncated our correlations to span the data from 1983 to 1930 for two reasons. The first being that our precipitation record, which we determined is the climatic process that dictates coral $\delta^{18}O$, decreases from 4 to 2 rain gauges at 1930. Secondly, the coral $\delta^{18}O$ becomes temporarily anti-correlated to the decadal component of the PDO (DPDO) during this time. The parenthetical values were calculated over the entirety of the given record. The direct relationship between seasonal coral $\delta^{18}O$ and precipitation averages suggests that during rainier wet seasons, the following dry seasons are also wetter. R-values are significant to the $p < 0.001$ level unless italicized.

	S1 Annual Average $\delta^{18}O$ (Decadal)		S1 Wet Season $\delta^{18}O$ (Decadal)	S1 Dry Season $\delta^{18}O$ (Decadal)
Precipitation (Decadal)	−0.58 (*−0.19*)	S1 Wet Season $\delta^{18}O$ (Decadal)	1	0.69 (0.58)
DPDO	0.73 (0.50)	S1 Dry Season $\delta^{18}O$ (Decadal)	0.69 (0.58)	1
AMO (Decadal)	−0.30 (*0.01*)	Precipitation (Decadal)	−0.62 (−0.46)	−0.46 (*0.12*)
		DPDO	0.66 (0.51)	0.54 (0.34)

5.2. Seasonality in $\delta^{18}O$-inferred precipitation

In examining the seasonal hydrologic budget of Panamá it is important to note that moisture flux to the region is impacted by variability emanating out of both the Pacific and Atlantic basins (Benway and

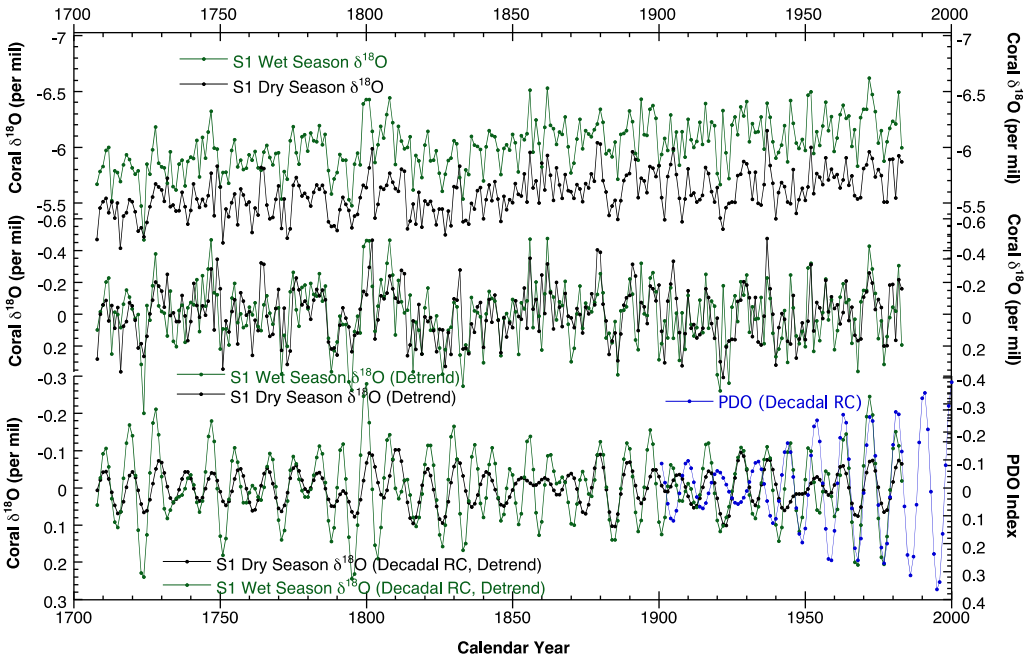

Fig. 7. In the top panel we separated the raw sub-annual S1 $\delta^{18}O$ into separate annual wet and dry season averages and illustrated that following wetter wet seasons the proceeding dry season was milder and had more rainfall than the average. The middle panel shows the detrended seasonal averages. For the entirety of the S1 $\delta^{18}O$ record the wet and dry season averages yielded a correlation coefficient of $R = 0.60$ ($p < 0.001$). The association between the wet and dry seasons could indicate that during more intense wet seasons the ITCZ is held farther north longer, the drainage basin has a delayed memory effect for it to return to typical conditions, or a combination of both. In the bottom panel we compared the decadal RC extracted from the wet and dry season averages to the corresponding band in the PDO. The wet season is very strongly correlated to the PDO, yielding a correlation coefficient of $R = 0.51$ ($p < 0.001$) ($R = 0.66$, $p < 0.001$ from present back to 1930), which supports our assertion that decadal variability in precipitation are dictated by the PDO. There is also a clear relationship with the dry season yielding a correlation coefficient of $R = 0.34$ ($p < 0.001$) ($R = 0.54$, $p < 0.001$ from present back to 1930).

Mix, 2004; Mestas-Nuñez et al., 2007; Lachniet et al., 2007, Lachniet, 2009). Atmospheric moisture that evaporates from warm Caribbean surface waters is seasonally transported over the isthmus where it precipitates over Central America and the eastern Pacific Ocean. About 0.1–0.3 Sv of freshwater is transported annually from the Atlantic to the Pacific via cross-isthmus vapor transport (Prange et al., 2010; Zaucker and Broecker, 1992). This net export of freshwater makes the surface of the tropical and subtropical Atlantic relatively salty, which may be a major influence on meridional overturning circulation by preconditioning North Atlantic surface waters before they move north (Prange et al., 2010).

Earlier studies examined the isotopic fingerprint of precipitation over the Panamá Bight in an effort to determine its source and better understand the Atlantic-Pacific teleconnection. Pacific-sourced moisture transport dominates during the rainy season (boreal summer and autumn) when the ITCZ is in its most northerly position (Prange et al., 2010). During the dry season, cross-isthmus transport increases and Atlantic-sourced moisture is transported while the ITCZ is more southerly and the northeasterly trades are strong (Prange et al., 2010, Brienen et al., 2012; Gloor et al., 2013). This leads to more upwelling and potential advection of cold water from the Gulf of Panamá. The $\delta^{18}O$ of precipitation decreases with increasing distance from the Caribbean Sea (Benway and Mix, 2004), therefore dry season precipitation has higher $\delta^{18}O$ than Pacific-sourced rain in the wet season. Thus, coral $\delta^{18}O$ is influenced by this source-effect in the same direction as the amount-effect. Ultimately precipitation and runoff into the Gulf of

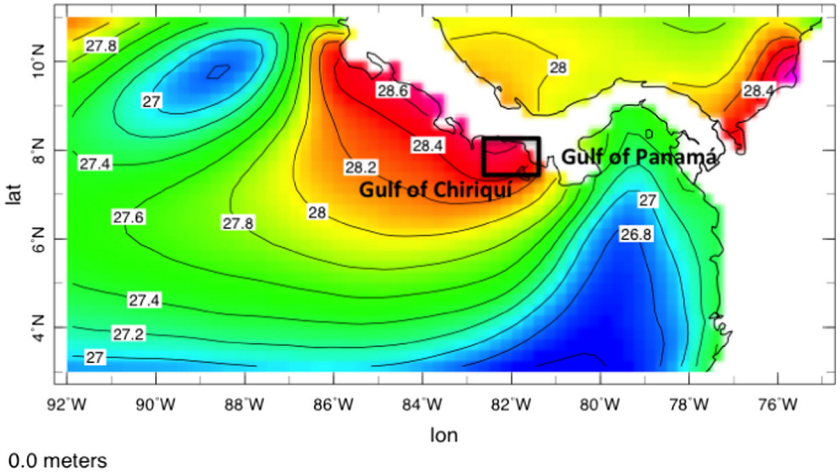

Fig. 8. Pacific Panamá's spatial distribution of average SST from 1981 to 2014, based on the OISST database. The spatial SST pattern shows distinct differences between the Gulfs of Chiriquí (warm) and Panamá (cool) from the upwelling of deep, cold water. Secas Island is located within the black box in the Gulf of Chiriquí.

Chiriquí can be influenced by changes in the ITCZ position over the eastern Pacific and Panamá as well as moisture flux from the Caribbean.

As expected, the average $\delta^{18}O$ wet season values are lower than the dry season averages. In the decadal band there is a significant relationship ($R = 0.58$, $p < 0.001$) between wet and dry season values in a given year. The wet seasons with particularly low $\delta^{18}O$ values were associated with dry seasons that also recorded low $\delta^{18}O$ (Fig. 7). A question is whether the dry season following a particularly rainy wet season is wetter than a normal (average) dry season or if the relationship in coral $\delta^{18}O$ is responding solely to a memory effect or delay in the Gulf of Chiriquí basin drainage? A comparison of average wet and dry season precipitation from the monthly rainfall dataset extending back to 1900 revealed that the relationship found in coral $\delta^{18}O$ exists in the seasonal average records of monthly instrumental rainfall data as well ($R = 0.74$, $p < 0.001$ from 1994 to 1901). This suggests that during particularly rainy wet seasons the ITCZ may be held farther north for longer, creating wetter than normal conditions during the typically dry months following the wet season. However, we cannot rule out the presence of a hydrologic memory effect in the drainage basin since the Pacific coast of Panamá is dotted with multiple rivers emptying into the Gulf of Chiriquí.

5.3. Decadal scale variability in $\delta^{18}O$

The origin of the pronounced decadal-scale mode in Secas Island coral $\delta^{18}O$ was not resolved by Linsley et al. (1994). Decadal variance was concentrated near a period of 9 years, but shown to vary from ~7 to ~11 years over the length of the 277 year long record. Less pronounced and regular multi-decadal variance in S1 coral $\delta^{18}O$ was also present (Linsley et al., 1994). Since there was no similar decadal component in instrumental SST and there is a decadal mode in regional rainfall (see Fig. 6) and perhaps also in instrumental SSS (see Linsley et al., 1994) we determined that the 9–12 year variability in S1 coral $\delta^{18}O$ was due to precipitation and river discharge, collectively hydrology. Linsley et al. (1994) ruled out direct forcing via the solar cycle since there was no clear correlation between the number of sunspots and precipitation or coral $\delta^{18}O$. Here we explore the origin of this decadal mode in coral $\delta^{18}O$ in more detail.

SSA of annual average regional precipitation data for the Pacific coast of Panamá isolated a decadal cycle which tracked the corresponding coral decadal RC moderately well with a correlation coefficient of $R = -0.58$ ($p < 0.001$) from 1984 back to 1930, (Fig. 6A). We incorporated multiple RCs (see Table 2) to develop the decadal component. SSA output of annual average coral $\delta^{18}O$ yielded a 9 year cycle (eigenvectors 1, 2) and an 11 year mode (eigenvector 15, 16) totaling 15% variance. The prominence and persistence of these cycles over multiple M-values (window lengths) suggests that the decadal mode comprises a significant part of the $\delta^{18}O$ variance. The presence of a decadal component in precipitation in accord with the corresponding decadal coral $\delta^{18}O$ band suggests that this mode of variability is related to the ITCZ. Additionally, the particularly wet interval in the early 1970s, evident in the instrumental record (Fig. 3B), proves to be regional in its scope as evidenced by an Amazon River tributary discharge record and an Amazonian tree ring $\delta^{18}O$ record (Brienen et al., 2012). Both records point to an increase in precipitation during this interval (Brienen et al., 2012). Later modeling work by Gloor et al. (2013) on the Amazonian catchment further supports the decadal hydrologic pattern, suggesting that this wet phase from the 1970s-1990s may not be solely driven by the ITCZ.

Decadal changes in North Pacific SST and associated ocean–atmosphere variability is the result of a series of inter-related extratropical and tropical processes that collectively have been captured (quantified) in the PDO Index (Newman et al., in press). Instrumental SST data indicate that interdecadal climate variability over much of the Pacific Ocean was coherent in the twentieth century. In the North Pacific this variability is termed the Pacific Decadal Oscillation (PDO) (Mantua et al., 1997; Zhang et al., 1997). Including data from the South Pacific, Power et al. (1999); Deser et al. (2004) and Folland et al. (2002) refer to the decadal SST variability as the Interdecadal Pacific Oscillation (IPO). Recently, the sum of the subtropical and equatorial processes responsible for the IPO-PDO pattern in Pacific SST has been linked to changes in global temperatures (Trenberth and Fasullo, 2013, Dai, 2013; among others) apparently via its effect on heat storage in the upper water column of the Pacific. This linkage is created in part by decadal changes in trade wind-driven shallow meridional overturning circulation (England et al., 2014).

The IPO-PDO phases are two to three decades in length. Positive IPO-PDO phases are associated with warming in the eastern Pacific and cooling in the central gyre regions with lower than average sea level pressure in the North Pacific (Mantua and Hare, 2002). During the negative phase of the IPO-PDO the SST and sea level pressure temporal patterns reverse yielding warming in the Central Pacific gyres, cooler SSTs along the North American coast and higher sea level pressure in the North and South Pacific. IPO-PDO extremes are further expressed as anomalously warm (negative phase) or cold (positive phase) conditions in the central Pacific Ocean gyres north and south of 20°. Central gyre temperatures are likely one of the most important determinants of the IPO-PDO that can influence the decadal phase of ITCZ-driven precipitation. The instrumental SST-based N. Pacific PDO index recorded negative phases from 1890 to 1924, 1947–1976 and after 1999, and positive phases from 1925 to 1946 and 1977 to ~1998 (Mantua et al., 1997 and updates).

The results of Newman et al. (in press) highlight the importance of tropical and extratropical processes in shaping the PDO (and IPO) and suggest that variability operating at both decadal and interdecadal-scales are involved. While the PDO phase is defined based on north Pacific SSTs, SST variability in the North Pacific is the end result of the coalescence of basin-wide phenomenon that may also dictate climate into the parts of North America (see: D'Arrigo et al., 2001; Graham, 1994; Latif and Barnett, 1994; Nigam et al., 1999; Dai, 2013). Our SSA of the annual average instrumental PDO Mantua and Hare index with a series of different M-values (window lengths) identified a stable set of RCs with mean periods of 9 years, a subset of total PDO variance (Table 1). We elected to isolate this decadal mode of the PDO (hereafter termed DPDO) by averaging all RCs from 9 to 12 years for comparison to the corresponding S1 coral $\delta^{18}O$ decadal RCs (Figs. 6, 7). The decadal phase in S1 $\delta^{18}O$ and the DPDO are moderately correlated yielding an $R = 0.51$ ($p < 0.001$) for the entire interval of overlap. The relationship between the two is reduced due to the misalignment from 1900 to 1930, which, if omitted, yields a stronger correlation of $R = 0.73$ ($p < 0.001$).

There is a complex system of ocean–atmosphere interactions linking the tropics and the subtropics that are captured in the PDO index. Newman et al. (in press) deconstruct the PDO into 3 main dynamical processes influencing SST in the North Pacific, Central Tropical Pacific, and Eastern Tropical Pacific, whose sum produces a reconstructed index that simulates PDO observations. As discussed below, the decadal band extracted from our coral $\delta^{18}O$ record may be responding to the influences of the equatorial Pacific variability that contribute to the total PDO regime.

El Niño events in Panamá are characterized by warm and dry conditions, making them difficult to identify in coral $\delta^{18}O$. While the Gulf of Chiriquí coral $\delta^{18}O$ record may not be an accurate archive of individual El Niño events, the DPDO, which influences coral $\delta^{18}O$ via precipitation may speak to low frequency patterns in eastern tropical Pacific climate phenomenon. If our DPDO is related to the eastern tropical component of the PDO as defined by Newman et al. (in press) we would expect to see a relationship with low frequency ENSO. We extracted the decadal component of the annually averaged Niño3.4 SST index (from Kaplan et al., 1998) in an effort to better define the DPDO. The DPDO and the decadal component of Niño3.4 were weakly correlated ($R = 0.31$,

$p < 0.001$), suggesting that the DPDO and lower frequency SST on the equator are at least in-part related, supporting the new multi-sourced variability theory (Newman et al., in press). The tropical variability embedded in the PDO influences the eastern Pacific ITCZ on decadal timescales and is linked to the total PDO index through an atmospheric bridge connecting the tropics with the extratropics. Our comparison of the DPDO with the decadal phase of Panamanian precipitation shows that more negative excursions in the DPDO index are indicative of wetter conditions. Applying that link to the DPDO-Nino3.4 relationship we determined that warmer Nino3.4 values were synonymous with drier periods in Panamá and likely more frequent or extended El Niño events led to periods of prolonged drought.

The DPDO has been examined in other literature but the manifestation of its influence on climate proxies varies. Dassié et al., 2014 also isolated the DPDO and combined it with an interdecadal phase and found a direct relationship with the decadal/interdecadal component in a Fijian coral $\delta^{18}O$ composite record, yielding a correlation coefficient of $R = 0.36$. They also found that decadal/interdecadal components in coral $\delta^{18}O$ track other climate indices (e.g. SOI, $R = -0.59$) in the south Pacific. It is not unprecedented for coral geochemistry to be an archive of low frequency climate oscillations and speaks to the complex nature of coral paleoceanographic records.

The strength of the decadal variability embedded within the PDO fluctuates through time. The D'Arrigo et al. (2001) tree ring PDO reconstruction may suggest that the DPDO's prominence changed through time. According to the study a shift towards more interannual/ENSO-type variability comprised most of the PDO variance from the mid 1800s until the 1976–77 PDO regime change (Villalba et al., 2001; D'Arrigo et al., 2001). After this shift to the positive PDO phase the decadal component regained its earlier prominence (D'Arrigo et al., 2001). The oscillation in the dominating mode of variability in the PDO index supports the view that it is a compilation of basin-wide processes operating on different timescales.

Establishing that S1 coral $\delta^{18}O$ and the DPDO are related suggests that local hydroclimate along Pacific Panamá varies with the PDO. The decadal component in the annual average DPDO Index and decadal variability in Panamanian rainfall were strongly correlated ($R = -0.62$, $p < 0.001$) back to 1930, at which point our precipitation composite shrinks from 4 to 2 stations. This suggests that the DPDO influences ITCZ-driven eastern tropical rainfall, which is archived in the coral geochemistry. However, the correlation for the entire record was slightly reduced to a moderate correlation ($R = -0.42$, $p < 0.001$), which may be due to the reduction in the number of rain gauges or a disturbance in the typical hydroclimate.

In addition to the relationship with Pacific variability, annual average S1 coral $\delta^{18}O$ exhibits an inverse relationship with the Atlantic Multidecadal Oscillation (AMO), albeit weaker than with the PDO. The AMO is the detrended anomaly of average SSTs in the North Atlantic Ocean (Gray et al., 2006; Lachniet et al., 2007). Previous reanalysis and modeling studies (e.g. Alexander et al., 2014; Kang et al., 2014) show that stronger than typical trade winds and warmer air over the western tropical Pacific is frequently accompanied by positive AMO and negative IPO-PDO phases (England et al., 2014). During extended, strongly positive AMO phases, the ITCZ is held northward, exposing Panamá to prolonged rainfall (Schneider et al., 2014). The decadal component of the AMO slightly leads the decadal component in the PDO. However, when the decadal RC of the AMO is more positive it is coincident with minima in the PDO decadal reconstructed component (Fig. 6C). Panamá's hydroclimate is multifaceted, influenced by variability originating from both the Atlantic and Pacific basins, however the AMO's influence is swamped in comparison to the PDO's control over annual rainfall, particularly the wet season.

From 1900 to 1930 the decadal cycle in S1 $\delta^{18}O$ is poorly correlated to the corresponding bands in precipitation and PDO. Changes in the decadal component in Panamanian precipitation and the DPDO are poorly correlated to S1 $\delta^{18}O$ during that period and the S1 wet and dry season averages exhibit asynchrony as well. To better understand this period of discord we revisited our age models and X-rays to corroborate the placement of our sampling paths and also determined that no track jumps or core breaks occurred near the interval in question. While these findings don't completely rule out chronology issues it is not likely that one could account for such a shift, particularly because the coral $\delta^{18}O$ decadal reconstructed components are in accord with precipitation before and after the 1900–1930 mismatch period (Fig. 6). In addition to revisiting our age models, we examined the decadal bands in annual average regional instrumental precipitation, the PDO, and the AMO all with independent chronologies, which revealed reduced amplitudes and a change in the phase relationship between the three indices. Ultimately, 1900–1930 appears to be a climatically confusing period for decadal variability relative to the mid-to-late 20th century. In this interval our analysis indicates that the: 1.) The strength (i.e. amplitude) in both the DPDO and the decadal band in the AMO is reduced. 2.) The consistent mid-to-late 20th century phasing between the PDO and AMO with the slight lead in the AMO changes, and 3.) The annual average decadal RC in regional precipitation is also less straightforward, temporarily aligning with neither the DPDO nor AMO. The transient dissolution of the PDO-AMO relationship in the 1900–1930 period and the simultaneous change in the influence on regional precipitation is a likely candidate for the coral $\delta^{18}O$-precipitation asynchrony. Additionally, we speculate that this interval of discord between the S1 and precipitation decadal RCs may have been due to a shift in the dominant climate forcing on $\delta^{18}O$ such as an influence from upwelling in the Gulf of Panama and its subsequent SST variability.

In an effort to more precisely determine the climate phenomena likely controlling the decadal variability in Panamanian precipitation we separately analyzed wet and dry season $\delta^{18}O$ values from the S1 coral $\delta^{18}O$ record using SSA. The DPDO is strongly correlated to the corresponding oscillation in the wet season $\delta^{18}O$ ($R = 0.66$, $p < 0.001$), omitting 1900–1930. This supports our assertion that on decadal timescales coral $\delta^{18}O$, is responding largely to changes in precipitation and that the spatial SST patterns associated with PDO influence precipitation in Panamá. We originally expected that the wet season variability would be controlled by the PDO and the dry season most influenced by the AMO, based on the contributing vapor source. Although this premise held true for the wet season it was not the case for the dry months. The comparisons between the decadal phases in the AMO with S1 seasonal $\delta^{18}O$ averages did not yield any significant correlations Additionally, we suspect that annual average coral $\delta^{18}O$ represents an integrated signal resulting from regional Panamanian precipitation, since the decadal phases in the AMO and precipitation were moderately correlated ($R = 0.53$, $p < 0.001$). The decadal phase in the AMO was weakly correlated to the corresponding RC in annual average S1 $\delta^{18}O$ (-0.30, $p < 0.001$) and only when the 1900–1930 period was omitted. A significant relationship would support the recent studies that suggest the positive AMO phase is indicative of warmer Atlantic SSTs and is correlated with precipitation along the Pacific coast of Panamá and an ITCZ held further north over the Eastern Tropical Pacific (see Alexander et al., 2014; England et al., 2014; Kang et al., 2014; Schneider et al., 2014). Our coral $\delta^{18}O$ record, however, only subtly tracks AMO variability.

The relationship between the DPDO and the decadal variability in precipitation also becomes unclear in the early 20th century, which suggests that this period was a time of climatic disorganization in the eastern tropical Pacific. This mismatch may have been the product of a weakened decadal cycle in the PDO, when we observe a decreased amplitude in the 1905–1925 CE window, which translates to a less pronounced temperature-driven decadal cycle in precipitation and therefore a less prominent decadal record in coral $\delta^{18}O$. A recent modeling study (see Steinman et al., 2015) shows that in the early 20th century, while the DPDO was weak and decoupled from coral $\delta^{18}O$ the AMO was more influential. However, from the late 20th to 21st centuries the AMO lost some of its previous power and the PDO grew in dominance (Steinman et al., 2015). The interplay between the fluctuating

variability emanating from both the Atlantic and Pacific basins controls low frequency variability in the hydrologic cycle on the Pacific since of Panamá.

6. Conclusions

The S1 coral $\delta^{18}O$ record presented in this study in conjunction with analysis of regional precipitation, the DPDO, and AMO allows for a more robust interpretation of variability in Panamanian precipitation along the Pacific coast than was originally presented in Linsley et al. (1994). We assert that decadal variation in coral $\delta^{18}O$ responds to ITCZ-driven precipitation as dictated by the DPDO, which may be a function of the eastern tropical Pacific subset of variability of the PDO. When the decadal oscillation in the PDO weakens the regional precipitation cannot drive decadal coral $\delta^{18}O$ throughout the Gulf of Chiriquí forcing the coral response to dissociate from rainfall. Future efforts should be undertaken to further understand the teleconnections between the Pacific and Atlantic basins and their association with coral $\delta^{18}O$ as well as with rainfall variability in Panamá on decadal time scales. Analysis of additional corals nearby Secas Island, supplemented with tree ring records, would also create a more robust portrayal of regional precipitation patterns by providing a denser network of data. Identifying the multiple unique sources of variability emanating from the Atlantic and Pacific basins influencing the decadal cycle in $\delta^{18}O$-inferred precipitation can enhance and improve regional climate models by providing more specific temporal parameters.

Acknowledgements

Funding for this work was provided in part by Lamont-Doherty Earth Observatory's Chevron Student Initiative Fund and the Lamont Climate Center with graduate student support from the National Science Foundation Graduate Student Research Fellowship DGE-11-44155.

References

Alexander, M.A., Kilbourne, K.H., Nye, J.A., 2014. Climate variability during warm and cold phases of the Atlantic multidecadal oscillatio (AMO) 1871-2008. J. Mar. Syst. 133, 14–26. http://dx.doi.org/10.1016/jmarsys.2013.07.017.

Alory, G., Maes, C., Delcroix, T., Reul, N., Illig, S., 2012. Seasonal dynamics of sea surface salinity off Panama: the far Eastern Pacific warm Pool. J. Geophys. Res. 117 (C4), C04028. http://dx.doi.org/10.1029/2011JC007802.

Benway, H.M., Mix, A.C., 2004. Oxygen isotopes, upper-ocean salinity, and precipitation sources in the eastern tropical Pacific. Earth Planet. Sci. Lett. 224 (3–4), 493–507. http://dx.doi.org/10.1016/j.epsl.2004.05.014.

Brienen, R.J.W., Helle, G., Pons, T.L., Guyot, J., Gloor, M., 2012. Oxygen isotopes in tree rings are a good proxy for Amazon precipitation and El Niño-Southern Oscillation variability. Proc. Natl. Acad. Sci. 109 (42), 16957–16962. http://dx.doi.org/10.1073/pnas.1205977109.

Cobb, K.M., Westphal, N., Sayani, H.R., Watson, J.T., Di Lorenzo, E., Cheng, H., Edwards, R.L., Charles, C.D., 2013. Highly variable El Niño-Southern Oscillation throughout the Holocene. Science 339 (6115), 67–70. http://dx.doi.org/10.1126/science.1228246.

Cole, J.E., Fairbanks, R.G., Shen, G.T., 1993. Recent variability in the Southern Oscillation: isotopic results from a Tarawa atoll coral. Science 260 (5115), 1790–1793. http://dx.doi.org/10.1126/science.260.5115.1790.

Dai, A., 2013. The influence of the inter-decadal Pacific oscillation on US precipitation during 1923–2010. Climate Dynamics 41, 633–646. http://dx.doi.org/10.1007/s00382-012-1446-5.

D'Arrigo, R.D., Villalba, R., Wiles, G., 2001. Tree-ring estimates of Pacific decadal climate variability. Clim. Dyn. 18 (3-4), 219–224. http://dx.doi.org/10.1007/s003820100177.

Dassié, E.P., Linsley, B.K., Corrège, T., Wu, H.C., Lemley, G.M., Howe, S., Cabioch, G., 2014. A Fiji multi-coral $\delta^{18}O$ composite approach to obtaining a more accurate reconstruction of the last two-centuries of the ocean-climate variability in the South Pacific Convergence Zone region. Paleoceanography 29. http://dx.doi.org/10.1002/2013PA002591 (18 pp.).

D'Croz, L., O'Dea, A., 2007. Variability in upwelling along the pacific shelf of Panama and implications for the distribution of nutrients and chlorphyll. Estuar. Coast. Shelf Sci. 73 (1–2). http://dx.doi.org/10.1016/j.ecss.2007.01.013.

D'Croz, L., O'Dea, A., 2009. Nutrient and Chlorophyll Dynamics in Pacific Central America (Panama). Proc. Smithson. Mar. Sci. Symp. (38), 335–344.

Delcroix, T., Alory, G., Cravatte, S., Corrège, T., McPhaden, M.J., 2011. A gridded sea surface salinity data set for the tropical Pacific with sample applications (1950-2008). Deep-Sea Res. I 58 (1), 38–48. http://dx.doi.org/10.1016/j.dsr.2010.11.002.

Deser, C., Ohillips, A.S., Hurrell, J.W., 2004. Pacific interdecadal climate variability: linkages between the tropics and the North Pacific during boreal winter since 1900. J. Clim. 17, 3109–3124.

Duque-Caro, H., 1990. Neogene stratigraphy, paleoceanography and paleobiogeography in northwest Southern America and the evolution of the Panama seaway. Palaeogeogr. Palaeoclimatol. Palaeoecol. 77 (3–4), 203–234. http://dx.doi.org/10.1016/0031-0182(90)90178-A.

England, M.H., McGregor, S., Spence, P., Meehl, G.A., Timmerman, A., Cai, W., Sen Gupta, A., McPhaden, M.J., Purich, A., Santoso, A., 2014. Recent intensification of wind-driven circulation in the Pacific and the ongoing warming hiatus. Nat. Clim. Chang. 4, 222–227. http://dx.doi.org/10.1038/nclimate2106.

Epstein, S., Buschsbaum, R., Lowenstam, H.A., Urey, H.C., 1953. Revised carbonate-water isotopic temperature scale. Geol. Soc. Am. Bull. 64 (11), 1315–1326. http://dx.doi.org/10.1130/0016-7606(1953)64[1315:RCITS]2.0.CO;2.

Evans, J.D., 1996. Straightforward Statistics for Behavioral Scientists. Brooks/Cole, Pacific Grove.

Fairbanks, R.G., Evans, M.N., Rubenstone, J.L., Broad, K., Moore, M.D., Charles, C.D., 1997. Evaluating climate indices and their geochemical proxies measured in corals. Coral Reefs 16, 93–100.

Folland, C.K., Renwick, J.A., Salinger, M.J., Mullan, A.B., 2002. Relative influences of the Interdecadal Pacific Oscillation and ENSO on the South Pacific Convergence Zone. Geophysical Research Letters 29 (13), 21-1–21-4. http://dx.doi.org/10.1029/2001GL014201.

Fukunaga, K., 1970. Introduction to Statistical Pattern Recognition. Academic Press, New York.

Gloor, M., Brienen, R.J.W., Galbraith, D., Feldpausch, T.R., Schöngart, J., Guyot, J.L., Espinoza, J.C., Lloyd, J., Phillips, O.L., 2013. Intensification of the Amazon hydrological cycle over the last two decades. Geophys. Res. Lett. 40 (9), 1729–1733. http://dx.doi.org/10.1002/grl.50377.

Glynn, P.W., 1977. Coral growth in upwelling and nonupwelling areas off the Pacific coast of Panama. J. Mar. Res. 35, 567–585.

Glynn, P.W., 1983. Extensive "bleaching' and death of reef corals on the Pacific coast of Panama. Environ. Conserv. 10 (2), 149–154. http://dx.doi.org/10.1017/S0376892900012248.

Graham, N., 1994. Decadal-scale climate variability in the 1970s and 1980s: observations and model results. Clim. Dyn. 10 (3), 135–162. http://dx.doi.org/10.1007/BF00210626.

Gray, S.T., Graumlich, L.J., Betancourt, J.L., Pederson, G.T., 2006. A tree-ring based reconstruction of the Atlantic Multidecadal Oscillation since 1567 AD. Geophys. Res. Lett. 31, L12205. http://dx.doi.org/10.1029/2004GL019932.

Horel, J.D., 1982. On the annual cycle of the tropical Pacific atmosphere and ocean. Mon. Weather Rev. 110, 1863–1878.

Howell, P., Pisias, N., Ballance, K., Baughman, J., Ochs, L., 2006. ARAND Time-Series Analysis Software. Brown University, Providence RI.

Hulme, M., 1992. A 1951-80 global land precipitation climatology for the evaluation of general circulation models. Clim. Dyn. 7 (2), 57–72. http://dx.doi.org/10.1007/BF00209609.

Hulme, M., 1994. Validation of Large-Scale Precipitation Fields in General Circulation Models. In: Desbois, M., Desalmand, F. (Eds.), Global Precipitations and Climate ChangeNATO ASI Series. Springer-Verlag, Berlin, pp. 387–406.

Kang, I.-S., No, H.-H., Kucharski, F., 2014. ENSO amplitude modulation associated with the mean SST Changes in the tropical central pacific induced by Atlantic multidecadal oscillation. J. Clim. 27 (20), 7911–7920. http://dx.doi.org/10.1175/JCLI-D-14-00018.1.

Kaplan, A., Cane, M.C., Kushnir, Y., Clement, A., Blumenthal, M., Rajagopalan, B., 1998. Analyses of global sea surface temperature 1856-1991. J. Geophys. Res. 103 (18), 18,567–18,589.

Kiladis, G.N., Diaz, H.F., 1989. Global climatic anomalies associated with extremes in Southern Oscillations. J. Clim. 2, 1069–1090.

Kumar, A., Yang, F., Goddard, L., Schubert, S., 2003. Differing trends in the tropical surface temperatures and precipitation over land and oceans. J. Clim. 17 (3), 653–664. http://dx.doi.org/10.1175/15200442(2004)017<0653:DTITTS>2.0.CO;2.

Lachniet, M.S., 2009. Sea Surface Temperature Control on the Stable Isotopic Composition of rainfall in Panama. Geophys. Res. Lett. 36, L03701. http://dx.doi.org/10.1029/2008GL036625, 2009.

Lachniet, M.S., Patterson, W.P., Burns, S., Asmerom, Y., Polyak, V., 2007. Caribbean and Pacific moisture sources on the isthmus of Panama revealed from stalagmite and surface water $\delta^{18}O$ gradients. Geophys. Res. Lett. 34, L01708. http://dx.doi.org/10.1029/2006GL028469.

Latif, M., Barnett, T.P., 1994. Causes of decadal climate variability over the North Pacific and North America. Science 266 (5185), 634–637. http://dx.doi.org/10.1126/science.266.5185.634.

Linsley, B.K., Dunbar, R.B., Wellington, G.M., Mucciarone, D.A., 1994. A coral-based reconstruction of intertropical convergence zone variability over Central America since 1707. J. Geophys. Res. 99 (C5), 9977–9994. http://dx.doi.org/10.1029/94JC00360.

Linsley, B.K., Kaplan, A., Gouriou, Y., Salinger, J., deMenocal, P.B., Wellington, G.M., Howe, S.S., 2006. Tracking the extent of the South Pacific convergence zone since the early 1600s, geochemistry, geophysics. Geosystems 7 (4), Q05003. http://dx.doi.org/10.1029/2005GC001115.

Mantua, N.J., Hare, S.R., 2002. The Pacific decadal oscillation. J. Oceanogr. 58 (1), 35–44. http://dx.doi.org/10.1023/A:1015820616384.

Mantua, N.J., Hare, S.R., Zhang, Y., Wallace, J.M., Francis, R.C., 1997. A Pacific interdecadal climate oscillation with impacts on Salmon Production. Bull. Am. Meteorol. Soc. 78 (6), 1069–1079. http://dx.doi.org/10.1175/1520-0477(1997)078<1069:APICOW>2.0.CO;2.

Mestas-Nuñez, A.M., Enfield, D.B., Zhang, D., 2007. Water vapor fluxes over the intra-Americas sea: seasonal and interannual variability and associations with rainfall.

J. Clim. 20 (9), 1910–1922. http://dx.doi.org/10.1175/1520-0477(1997)078<1069:APICOW>2.0.CO;2.
Newman, M., Alexander, M.A., Ault, T.R., Cobb, K.M., Deser, C., Di Lorenzo, E., Mantua, N.J., Miller, A.J., Minobe, S., Nakamura, H., Schneider, N., Vimont, D.J., Phillips, A.S., Scott, J.D., Smith, C.A., 2015. The Pacific decadal oscillation, revisited. J. Clim. (in press).
Nigam, S., Barlow, M., Berbery, E., 1999. Analysis links Pacific decadal variability to drought and streamflow in the United States. Eos 80 (51), 621–622 625.
Philander, S.G., 1990. El Niño, La Niña, and the Southern Oscillation. Academic Press, San Diego.
Poveda, G., Waylen, P.R., Pulwarty, R.S., 2006. Annual and inter-annual variability of the present climate in northern South America and southern Mesoamerica. Palaeogeogr. Palaeoclimatol. Palaeoecol. 234 (1), 3–27. http://dx.doi.org/10.1016/j.palaeo.2005.10.031.
Power, S.T., Casey, C., Folland, A., Colman, A., Mehta, V., 1999. Interdecadal modulation of the impact of ENSO on Australia. Clim. Dyn. 15, 319–324.
Prange, M., Steph, S., Schulz, M., Keigwin, L.D., 2010. Inferring moisture transport across Central America: can modern analogs of climate variability help reconcile paleosalinity records? Quat. Sci. Rev. 29 (11–12), 1317–1321. http://dx.doi.org/10.1016/j.quascirev.2010.02.029.
Ropelewski, C.F., Halpert, M.S., 1987. Global and regional scale precipitation associated with El Niño Southern oscillation. Mon. Weather Rev. 115, 1606–1626.
Ropelewski, C.F., Halpert, M.S., 1989. Precipitaiton patterns associated with the high-index phase of the Southern Oscillation. J. Clim. 2, 268–284.
Schneider, T., Bischoff, T., Haug, G.H., 2014. Migrations and dynamics of the intertropical convergence zone. Nature 513 (7516), 45–53. http://dx.doi.org/10.1038/nature13636.
Soden, B.J., Held, I.M., 2006. An assessment of climate feedbacks in coupled ocean–atmosphere models. J. Clim. 19 (14), 3354–3360. http://dx.doi.org/10.1175/JCLI3799.1.
Steinman, B.A., Mann, M.E., Miller, S., 2015. Atlantic and Pacific multidecadale oscillations and Northern Hemisphere temperatures. Science 347 (6225), 988–991. http://dx.doi.org/10.1126/science.1259435.
Trenberth, K.E., Fasullo, J.T., 2013. An apparent hiatus in global warming? Earth's Futur. 1 (1), 19–32. http://dx.doi.org/10.1002/2013EF000165.
Urban, F.E., Cole, J.E., Overpeck, J.T., 2000. Influence of mean climate change on climate variability from a 1550 year tropical Pacific coral record. Lett. Nat. 407, 989–993. http://dx.doi.org/10.1038/35039597.
Valiela, I., Camilli, L., Stone, T., Giblin, A., Crusius, J., Fox, S., Barth-Jensen, C., Monteiro, R.O., Tucker, J., Martinetto, P., Harris, C., 2012. Increased rainfall remarkably freshens estuarine an coastal waters on the Pacific coast of Panama: magnitude and likely effects on upwelling and nutrient supply. Glob. Planet. Chang. 92-93, 130–137. http://dx.doi.org/10.1016/j.gloplacha.2012.05.006.
Vautard, R., Ghil, M., 1989. Singular spectrum analysis in nonlinear dynamics with applications to paleoclimatic time series. Phys. D. Nonlinear Phenom. 35, 395–424.
Vautard, R., Yiou, R., Ghil, M., 1992. Singular-spectrum analysis: A toolkit for short, noisy, chaotic signals. Phys. D. Nonlinear Phenom. 58, 95–126.
Villalba, R., D'Arrigo, R., Cook, E., Jacoby, G., Wiles, G., 2001. Decadal-Scale Climate Variability along the Extratropical Western Coast of the Americas: Evidence from Tree-Ring Records. In: Markgraf, V. (Ed.), Interhemispheric Climate Linkages. American Meteorological Society.
Wellington, G.M., Glynn, P.W., 1983. Environmental influences on skeletal banding in eastern pacific (Panama) corals. Coral Reefs 1 (4), 215–222. http://dx.doi.org/10.1007/BF00304418.
Wellington, G.M., Dunbar, R.B., Merlen, G., 1996. Calibration of stable oxygen isotope signatures in Galápagos corals. Paleoceanography 11 (4), 467–480. http://dx.doi.org/10.1029/96PA01023.
Xie, P., Arkin, P.A., 1996. Analyses of global monthly precipitation using gauge observations, satellite estimates, and numerical model predictions. J. Clim. 9, 840–858.
Xie, P., Arkin, P.A., 1997. Global precipitation: A 17-year monthly analysis based on gauge observations, satellite estimates and numerical model outputs. BAMS 78, 2539–2558.
Zaucker, F., Broecker, W.S., 1992. The influence of atmospheric moisture transport on the fresh water balance of the Atlantic drainage basin: general circulation model simulations and observations. J. Geophys. Res. Atmos. 97 (D3), 2765–2773. http://dx.doi.org/10.1029/91JD01699.
Zhang, Y., Wallace, J.M., Battisti, D.S., 1997. ENSO-like interdecadal variability: 1900-93. J. Clim. 10 (5), 1004–1020. http://dx.doi.org/10.1175/1520-0442(1997)010<1004:ELIV>2.0.CO;2.